

Measurement of the Neutral Weak Form Factors of the Proton

K. A. Aniol,¹ D. S. Armstrong,²⁴ M. Baylac,²⁰ E. Burtin,²⁰ J. Calarco,¹³ G. D. Cates,¹⁷
C. Cavata,²⁰ J.-P. Chen,⁶ E. Chudakov,⁶ D. Dale,⁸ C. W. de Jager,⁶ A. Deur,^{6,2}
P. Djawotho,²⁴ M. B. Epstein,¹ S. Escoffier,²⁰ L. Ewell,¹¹ N. Falletto,²⁰ J. M. Finn,²⁴
K. Fissum,¹² A. Fleck,¹⁸ B. Frois,²⁰ J. Gao,¹² F. Garibaldi,⁵ A. Gasparian,³
G. M. Gerstner,²⁴ R. Gilman,¹⁹ A. Glamazdin,⁹ J. Gomez,⁶ V. Gorbenko,⁹ O. Hansen,⁶
F. Hersman,¹³ R. Holmes,²² M. Holtrop,¹³ B. Humensky,¹⁷ S. Incerti,²³ J. Jardillier,²⁰
M. K. Jones,²⁴ J. Jorda,²⁰ C. Jutier,¹⁶ W. Kahl,²² D. H. Kim,¹⁰ M. S. Kim,¹⁰ K. Kramer,²⁴
K. S. Kumar,¹⁷ M. Kuss,⁶ J. LeRose,⁶ M. Leuschner,¹³ D. Lhuillier,²⁰ N. Liyanage,¹²
R. Lourie,²¹ R. Madey,⁷ D. J. Margaziotis,¹ F. Marie,²⁰ J. Martino,²⁰ P. Mastromarino,¹⁷
K. McCormick,¹⁶ J. McIntyre,¹⁹ Z.-E. Meziani,²³ R. Michaels,⁶ G. W. Miller,¹⁷
D. Neyret,²⁰ C. Perdrisat,²⁴ G. G. Petratos,⁷ R. Pomatsalyuk,⁹ J. S. Price,⁶ D. Prout,⁷
V. Punjabi,¹⁴ T. Pussieux,²⁰ G. Quémener,²⁴ G. Rutledge,²⁴ P. M. Rutt,⁶ A. Saha,⁶
P. A. Souder,²² M. Spradlin,^{17,4} R. Suleiman,⁷ J. Thompson,²⁴ L. Todor,¹⁶ P. E. Ulmer,¹⁶
B. Vlahovic,¹⁵ K. Wijesooriya,²⁴ R. Wilson,⁴ B. Wojtsekhowski⁶
(HAPPEX Collaboration)

¹ *California State University - Los Angeles, Los Angeles, CA 90032,*

² *LPC, Université Blaise Pascal/IN2P3, F-63177 Aubière, France*

³ *Hampton University, Hampton, VA 23668*

⁴ *Harvard University, Cambridge, MA 02138*

⁵ *Istituto Nazionale di Fisica Nucleare, Sezione Sanità, 00161 Roma, Italy*

⁶ *Thomas Jefferson National Accelerator Laboratory, Newport News, VA 23606*

⁷ *Kent State University, Kent, OH 44242*

⁸ *University of Kentucky, Lexington, KY 40506*

⁹ *Kharkov Institute of Physics and Technology, Kharkov 310108, Ukraine*

¹⁰ *Kyungpook National University, Taegu 702-701, Korea*

¹¹ *University of Maryland, College Park, MD 20742*

¹² *Massachusetts Institute of Technology, Cambridge, MA 02139*

¹³ *University of New Hampshire, Durham, NH 03824*

¹⁴ *Norfolk State University, Norfolk, VA 23504*

¹⁵ *North Carolina Central University, Durham, NC 27707*

¹⁶ *Old Dominion University, Norfolk, VA 23508*

¹⁷ *Princeton University, Princeton, NJ 08544*

¹⁸ *University of Regina, Regina, SK S4S 0A2, Canada*

¹⁹ *Rutgers, The State University of New Jersey, Piscataway, NJ 08855*

²⁰ *CEA Saclay, DAPNIA/SPhN, F-91191 Gif-sur-Yvette, France*

²¹ *State University of New York at Stony Brook, Stony Brook, NY 11794*

²² *Syracuse University, Syracuse, NY 13244*

²³ *Temple University, Philadelphia, PA 19122*

²⁴ *College of William and Mary, Williamsburg, VA 23187*

(September 9, 2018)

Abstract

We have measured the parity-violating electroweak asymmetry in the elastic scattering of polarized electrons from the proton. The kinematic point ($\langle\theta_{\text{lab}}\rangle = 12.3^\circ$ and $\langle Q^2 \rangle = 0.48 \text{ (GeV/c)}^2$) is chosen to provide sensitivity, at a level that is of theoretical interest, to the strange electric form factor G_E^s . The result, $A = -14.5 \pm 2.2 \text{ ppm}$, is consistent with the electroweak Standard Model and no additional contributions from strange quarks. In particular, the measurement implies $G_E^s + 0.39G_M^s = 0.023 \pm 0.034 \text{ (stat)} \pm 0.022 \text{ (syst)} \pm 0.026 \text{ } (\delta G_E^n)$, where the last uncertainty arises from the estimated uncertainty in the neutron electric form factor.

13.60.Fz, 11.30.Er, 13.40.Gp, 14.20.Dh

The proton, which is believed to be a state of three quarks bound by the strong force of QCD, is a complex object when probed at intermediate energies. In order to develop a useful description, one must first establish all the relevant degrees of freedom. Recent theoretical and experimental investigations have indicated that strangeness might play an important role [1,2]. For example, do $s\bar{s}$ pairs contribute to the charge radius or magnetic moment of the proton? Quite possibly, since the mass of the strange quark is comparable to the proton mass and the scale of the strong interaction. On the other hand, the empirically successful OZI rule predicts that the effects of strange quarks are greatly suppressed at low energies [3]. Resolution of this issue requires that it be addressed experimentally.

A particularly clean experimental technique [4] for isolating the effects of strange quarks in the nucleon is measuring parity-violation amplitudes in the elastic scattering of polarized electrons from protons [5]. The theoretical asymmetry, which is caused by the interference between the weak and electromagnetic amplitudes, is given in the Standard Model by [2]

$$A_{th} = \frac{\sigma_R - \sigma_L}{\sigma_R + \sigma_L} = \left[\frac{-G_F Q^2}{\pi \alpha \sqrt{2}} \right] \quad (1)$$

$$\times \frac{\varepsilon G_E^{p\gamma} G_E^{pZ} + \tau G_M^{p\gamma} G_M^{pZ} - \frac{1}{2}(1 - 4 \sin^2 \theta_W) \varepsilon' G_M^{p\gamma} G_A^{pZ}}{\varepsilon (G_E^{p\gamma})^2 + \tau (G_M^{p\gamma})^2}$$

where $G_E^{p\gamma}$ ($G_M^{p\gamma}$) is the electric(magnetic) Sachs form factor for photon exchange, $G_{E,M}^{pZ}$ is the corresponding quantity for Z^0 exchange and θ_W is the electroweak mixing angle. All form factors are functions of Q^2 and ε , τ , and ε' are kinematic quantities (see Ref. [6]). For our kinematics, $\tau \sim 0.136$, $\varepsilon \sim .97$, $\varepsilon' \ll 1$ and the term involving G_A^{pZ} contributes only a few percent relative to the other terms. The predicted asymmetry is on the order of 10 parts per million (ppm).

To interpret the experiment, $G_{E,M}^{p,Z}$ can be expressed in terms of proton, neutron, and strange form factors if the up(down) quarks in the proton have the same properties as the down(up) quarks in the neutron (assumption of isospin symmetry). Then

$$G_{E,M}^{p,Z} = \frac{1}{4}(G_{E,M}^{p\gamma} - G_{E,M}^{n\gamma}) - \sin^2 \theta_W G_{E,M}^{p\gamma} - \frac{1}{4} G_{E,M}^s$$

and, if the electromagnetic form factors are sufficiently well known from experiment, the only unknown quantities involve strange form factors.

Extensive literature is devoted to estimating the size of strange form factors. Approaches include [2,3,7–11] pole fits, meson loops, the NJL model, vector dominance, unquenched quark model, chiral symmetry, and skyrme models. The significance of the strange form factors is attested to by the fact that they are relevant to many theoretical approaches striving to understand QCD at low energies. Some of the calculations predict substantial effects, 50% or more of the asymmetry at our kinematics, that are dominated by G_E^s . Other calculations predict effects at the few percent level or less. The goal of our experiment is to determine if indeed the strange quark form factors are large enough to be an important part of any detailed description of the proton.

The experiment took place in Hall A at the Thomas Jefferson National Accelerator Facility (JLab). A $\sim 100\mu\text{A}$ continuous-wave beam of longitudinally polarized 3.356 GeV

electrons was scattered from a 15 cm long liquid hydrogen target. The electrons which were scattered elastically at $\langle\theta_{\text{lab}}\rangle \sim \pm 12.3^\circ$ were focussed by two identical high resolution 5.5 msr spectrometers onto a total-absorption detector made up of a lead-lucite sandwich. Only the scattered electrons were detected; the second spectrometer merely doubled the solid angle. The spectrometers, which deflect the electrons by 45° out of the scattering plane, focus inelastic trajectories well away from our detectors.

The polarized electron beam originated from a bulk GaAs photocathode excited by circularly polarized laser light. The helicity of the beam was set every 33.3 ms locked to the 60 Hz frequency of the AC power in the lab. The helicity was structured as pairs of consecutive 33.3 ms periods with opposite helicity, henceforth called windows. The helicity of the first window in each pair was determined by a pseudo-random number generator. All signals were integrated over a 32 ms gate which began ~ 1 ms after the start of each window. The output of the integrators was digitized by 16-bit customized analog to digital converters. Integration and digitization were handled by custom-built modules designed to minimize noise and crosstalk.

The experimental method is driven primarily by the fact that the measured asymmetry is a few ppm. The trick to measuring small asymmetries is to maintain negligible correlations between the helicity of the beam and any other properties of the beam, such as intensity, energy, position, or angle. At JLab, the only quantity for which we found a non-zero helicity-correlated difference was intensity. This correlation was reduced to below 1 ppm by using a slow feedback system.

The intensity of the beam was measured with two independent RF cavities and the position of the beam was measured at five locations with RF stripline monitors. Window-to-window jitter in the intensity was typically 300 ppm and window-to-window jitter in position was a few microns. This impressive stability of the accelerated beam made it easy to set stringent limits on any helicity-correlated beam parameters. Averaged over the entire run, limits on the position differences were typically on the order of a few nm. One of the position monitors was located at a point of high dispersion in the transport line and set a limit on the average helicity-correlated fractional energy difference at the 10^{-8} level.

Limits on the impact of the helicity correlations were determined by modulating the beam position and energy concurrent with data taking. Since these changes were small and uncorrelated with helicity, the same data could be used both for calibration purposes as well as for the primary data sample. The results of these studies show that the contribution of the correlations to the raw asymmetry is a factor of 20 smaller than the statistical error and thus negligible.

The raw asymmetry for each window pair is defined

$$A_{\text{raw}} = [(D_R/I_R) - (D_L/I_L)]/[(D_R/I_R) + (D_L/I_L)],$$

where $D_R(D_L)$ is the detector signal and $I_R(I_L)$ is the signal from the intensity cavity for the right(left) helicity window. Pedestals for these signals were measured during beam-off periods and the linearity of the system was verified at the 1% level during periods when the beam current was ramping up. A histogram of the distribution of window pair asymmetries is given in Fig. 1. The distribution is purely Gaussian. Separate auxiliary tests (at lower beam energy and thus high cross section) carried out prior to the run demonstrated that boiling of the liquid target did not increase the noise in the asymmetry measurements. The

only cuts applied to our data sample were when the beam was $< 3\mu\text{A}$ or when equipment such as the spectrometer or target was clearly malfunctioning.

One important test for the presence of false asymmetries is through the insertion of a half-wave ($\lambda/2$) plate in the laser beam. This complements the helicity of the electron beam and hence the sign of the raw asymmetry while leaving many other possible systematic effects unchanged. The data were taken in sets of 24-48 hr duration, and the $\lambda/2$ plate was inserted for the odd numbered sets. The raw asymmetries for each set are given in Fig. 2. A clear correlation between the presence of the $\lambda/2$ plate and the sign of the asymmetry is seen. Since the target is unpolarized, this correlation is an unambiguous signal of parity violation. Averages of the raw asymmetries for the entire data set, representing 78 C of electrons on target, are given in Table I for both $\lambda/2$ plate settings and for each spectrometer individually. The results for the subsets are consistent with each other.

To extract the experimental asymmetry $A_{exp} = A_{raw}/P_e$, the beam polarization was measured both by Mott scattering near the injector and by Møller scattering just upstream of the hydrogen target. We use the average value $P_e = (0.388 \pm 0.027)$. The Q^2 of the data, averaged over the acceptance of the detector, was determined to be 0.479 ± 0.003 $(\text{GeV}/c)^2$ by separate low-current runs that used tracking drift chambers in front of our detectors to study individual events. The drift chambers were used also to measure possible inelastic backgrounds from pole-tip scattering by varying the central momentum of the spectrometers so that the dominant elastic events would follow the trajectories of inelastic events under running conditions. The contribution of background to our asymmetry is at most 2% of 15 ppm as listed in the summary of errors in Table II. The result is $A_{exp} = -14.5 \pm 2.0(stat) \pm 1.1(syst)$ ppm.

To study the effects of strange quarks, we compare our result with A_{th} (Eq. 1) using parameterizations of the form factors. For G_E^n we use the function due to Galster [12]. The difference between the true value and the Galster approximation is denoted δG_E^n . It is estimated to be $\pm 50\%$ of the Galster function, corresponding to a 9.6% error in A_{th} . We will leave this as a separate error since it is significant and since experiments in progress should improve the value of δG_E^n . For the other form factors, the dipole parameterization is taken as a reasonable approximation at our Q^2 : $G_E^p = G_D$, $G_M^p = \mu_p G_D$, and $G_M^n = \mu_n G_D$ [2]. This introduces an uncertainty in the predicted asymmetry of about 4% of itself. Electroweak radiative corrections [2,13], which are known and only on the order of a few percent of the asymmetry, were applied. The kinematic suppression of the G_A^Z term is essential in our experiment to control the otherwise large radiative corrections in that term. With these assumptions, $A_{th} = -15.8 \pm 0.7 \pm 1.5(\delta G_E^n)$ ppm.

Representative calculations for $\delta A = (A_{exp} - A_{th})/A_{th}$ are given in Fig. 3 together with our data point under the assumption that δG_E^n is negligible. The largest of the predictions are excluded by our data. Previous data sensitive to different combinations of the form factors and at different Q^2 values are also consistent with the absence of strange quarks, but at a somewhat less sensitive level [6,14]. From our data, we can extract the combination of strange form factors at $Q^2 = 0.48$ $(\text{GeV}/c)^2$: $G_E^s + 0.39G_M^s = 0.023 \pm 0.034$ (stat) ± 0.022 (syst) ± 0.026 (δG_E^n). Our result is shown in Fig. 4, expressed as the combination of strange form factors that we measure versus G_E^n .

We plan to improve our precision by a factor of 2 in 1999. Improvements in G_E^n will be important for us to extract useful information. Although we have ruled out some of the

more generous predictions, it is important to pursue the subject further. Expanding the Q^2 range is important, as well as separating G_E^s from G_M^s , either by varying the kinematics or by using an isoscalar target such as ^4He .

The relative ease with which we were able to measure the small asymmetry at JLab bodes well for the future of experiments measuring parity-violating amplitudes. The high quality of the beam provided by this new facility is invaluable for the performance of precision experiments.

We wish to thank the entire staff at JLab for their tireless work in developing this new facility, and particularly C. K. Sinclair and M. Poelker for their timely work on the polarized source. This work was supported, in part, by the Department of Energy, the National Science Foundation, the Korean Science and Engineering Foundation (Korea), the INFN (Italy), the Natural Sciences and Engineering Research Council of Canada, and the Commissariat à l'Énergie Atomique (France).

REFERENCES

- [1] D. B. Kaplan and A. Manohar, Nucl. Phys. **B310**, 527 (1988).
- [2] M. J. Musolf *et al.*, Phys. Rep. **239**, 1 (1994) and references therein.
- [3] P. Geiger and N. Isgur, Phys. Rev. D **55**, 299 (1997).
- [4] C. Y. Prescott *et al.*, Phys. Lett. **84B**, 524 (1979); W. Heil *et al.*, Nucl. Phys. **B327**, 1 (1989); P. A. Souder *et al.*, Phys. Rev. Lett. **65**, 694 (1990).
- [5] R. D. McKeown, Phys. Lett. B **219**, 140 (1989).
- [6] B. Mueller *et al.*, Phys. Rev. Lett **78**, 3824 (1997).
- [7] R. L. Jaffe, Phys. Lett. B **229**, 275 (1989).
- [8] M. J. Musolf and M. Burkhardt, Z. Phys. C **61**, 433 (1994).
- [9] H. Weigel *et al.*, Phys. Lett. B **353**, 20 (1995).
- [10] H. -W. Hammer, Ulf-G. Meissner, and D. Drechsel, Phys. Lett. B **367**, 323 (1996).
- [11] M. J. Ramsay-Musolf and H. Ito, Phys. Rev. C **55**, 3066 (1997).
- [12] S. Galster *et al.*, Nucl. Phys. **B32**, 221 (1971).
- [13] Particle Data Group, C. Caso *et al.*, Eur. Phys. J. C **3**, 1 (1998). The electroweak radiative corrections are essentially the same as for atoms. In addition, the peaking approximation is used to correct for the radiative tail.
- [14] G. T. Garvey *et al.*, Phys. Rev. C **48**, 1919 (1993).

TABLES

	$\lambda/2$ out	$\lambda/2$ in	Combined
det1	5.1 ± 1.4	-3.3 ± 1.6	-4.25 ± 1.06
det2	6.2 ± 1.5	-8.1 ± 1.6	-7.07 ± 1.07
Total	5.6 ± 1.0	-5.6 ± 1.1	-5.64 ± 0.75

TABLE I. Averages of A_{raw} (in ppm). The different spectrometers are det1 and det2.

A	Source of error	$\Delta A/A(\%)$
A_{raw}	Statistics	13.4
	Others	<0.3
A_{exp}	Beam Polarization	7
	Q^2 Determination	1
	Backgrounds	2
A_{th}	Nucleon Form Factors (excluding G_E^n)	4.0
	Radiative Corrections	1.4
	G_E^n	9.6

TABLE II. Summary of contributions to the errors for A_{raw} , A_{exp} , and A_{th} .

FIGURES

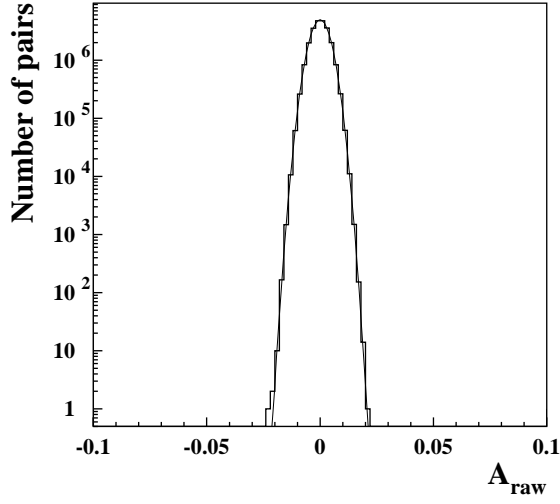


FIG. 1. Distribution of A_{raw} for individual window pairs. Only data with $I > 80\mu\text{A}$ ($\sim 95\%$ of sample) are shown. The curve is a Gaussian fit.

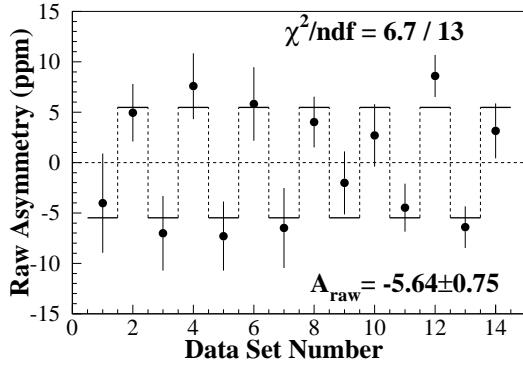


FIG. 2. Average values of A_{raw} for each data set. Odd data sets have the $\lambda/2$ plate inserted in the laser beam. The plate is expected simply to change the sign of the raw asymmetry.

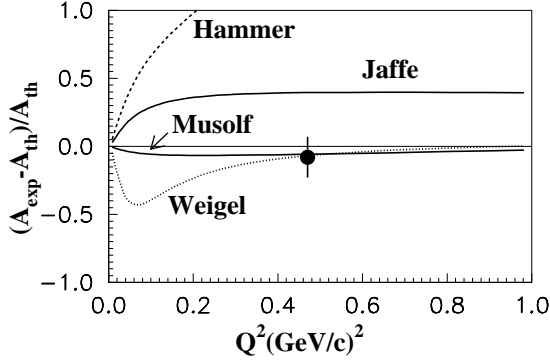


FIG. 3. Experimental $\delta A/A$ assuming $\delta G_E^n = 0$, together with representative theoretical calculations by Jaffe [7], Hammer *et al.* [10], Musolf and Burkhardt [8], and Weigel [9]. For papers that did not include the Q^2 dependence [7,8] a dipole form is assumed as suggested in Ref. [2].

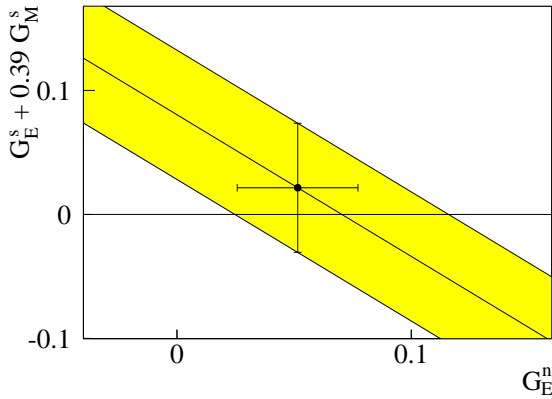


FIG. 4. Allowed region of space in $(G_E^s + 0.39G_M^s)$ versus G_E^n at $Q^2 = 0.48$ $(\text{GeV}/c)^2$. Data point assumes Galster approximation for G_E^n .